


RESEARCH ARTICLE

Histidine¹⁶⁸ is crucial for ΔpH-dependent gating of the human voltage-gated proton channel, hH_V1

Vladimir V. Cherny¹, Deri Morgan¹, Sarah Thomas², Susan M.E. Smith², and Thomas E. DeCoursey¹ 

We recently identified a voltage-gated proton channel gene in the snail *Helisoma trivolvis*, HtH_V1, and determined its electrophysiological properties. Consistent with early studies of proton currents in snail neurons, HtH_V1 opens rapidly, but it unexpectedly exhibits uniquely defective sensitivity to intracellular pH (pH_i). The H⁺ conductance (g_H)- V relationship in the voltage-gated proton channel (H_V1) from other species shifts 40 mV when either pH_i or pH_o (extracellular pH) is changed by 1 unit. This property, called ΔpH-dependent gating, is crucial to the functions of H_V1 in many species and in numerous human tissues. The HtH_V1 channel exhibits normal pH_o dependence but anomalously weak pH_i dependence. In this study, we show that a single point mutation in human hH_V1—changing His¹⁶⁸ to Gln¹⁶⁸, the corresponding residue in HtH_V1—compromises the pH_i dependence of gating in the human channel so that it recapitulates the HtH_V1 response. This location was previously identified as a contributor to the rapid gating kinetics of H_V1 in *Strongylocentrotus purpuratus*. His¹⁶⁸ mutation in human H_V1 accelerates activation but accounts for only a fraction of the species difference. H168Q, H168S, or H168T mutants exhibit normal pH_o dependence, but changing pH_i shifts the g_H - V relationship on average by <20 mV/unit. Thus, His¹⁶⁸ is critical to pH_i sensing in hH_V1. His¹⁶⁸, located at the inner end of the pore on the S3 transmembrane helix, is the first residue identified in H_V1 that significantly impairs pH sensing when mutated. Because pH_o dependence remains intact, the selective erosion of pH_i dependence supports the idea that there are distinct internal and external pH sensors. Although His¹⁶⁸ may itself be a pH_i sensor, the converse mutation, Q229H, does not normalize the pH_i sensitivity of the HtH_V1 channel. We hypothesize that the imidazole group of His¹⁶⁸ interacts with nearby Phe¹⁶⁵ or other parts of hH_V1 to transduce pH_i into shifts of voltage-dependent gating.

Introduction

Voltage-gated proton channels, H_V1, possess several distinctive or unique properties (DeCoursey, 2015). They are exquisitely proton selective with single-channel currents in the femtoampere range (Cherny et al., 2003). Perhaps because the conduction pathway is narrow and lacks a continuous water wire (Kulleperuma et al., 2013; Morgan et al., 2013; Chamberlin et al., 2014; Dudev et al., 2015), no high-affinity blockers exist that act by simple occlusion of the pore. The most potent inhibitor is Zn²⁺, which binds competitively with protons to two histidines in the external vestibule of human H_V1 (hH_V1) and interferes with channel opening (Cherny and DeCoursey, 1999; Takeshita et al., 2014). Although controversial (Bennett and Ramsey, 2017; DeCoursey, 2017), the conduction pathway includes an aspartate that appears to be obligatorily protonated and deprotonated during permeation (DeCoursey, 2003; Musset et al., 2011; Smith et al., 2011; Dudev et al., 2015; van Keulen et al., 2017). Consequently, H⁺ conduction has anomalously large temperature dependence (DeCoursey and

Cherny, 1998; Kuno et al., 2009) and deuterium isotope effects (DeCoursey and Cherny, 1997) when compared with other channels. H_V1 in many species are dimers (Koch et al., 2008; Lee et al., 2008; Tombola et al., 2008), but monomeric constructs also function with fairly subtle differences from the dimer (Koch et al., 2008; Tombola et al., 2008; Musset et al., 2010).

Perhaps the most unusual property of H_V1 is ΔpH-dependent gating, a unique mechanism that is essential to all its functions. Although H_V1 is a voltage-gated ion channel, the voltage at which all known H_V1 open is strongly dependent on pH. Increasing pH_o or decreasing pH_i shifts the H⁺ conductance (g_H)- V relationship negatively by ~40 mV/unit. At symmetrical pH (pH_o = pH_i), the threshold for activation in most species is 10–20 mV (Cherny et al., 1995; DeCoursey, 2013). The combination of these properties ensures that under almost all conditions encountered by living cells, H_V1 opens only when the electrochemical gradient for H⁺ is outward, so that opening H_V1 channels results in

¹Department of Physiology & Biophysics, Rush University, Chicago, IL; ²Department of Molecular and Cellular Biology, Kennesaw State University, Kennesaw, GA.

Correspondence to Thomas E. DeCoursey: tdcour@rush.edu.

© 2018 Cherny et al. This article is distributed under the terms of an Attribution–Noncommercial–Share Alike–No Mirror Sites license for the first six months after the publication date (see <http://www.rupress.org/terms/>). After six months it is available under a Creative Commons License (Attribution–Noncommercial–Share Alike 4.0 International license, as described at <https://creativecommons.org/licenses/by-nc-sa/4.0/>).

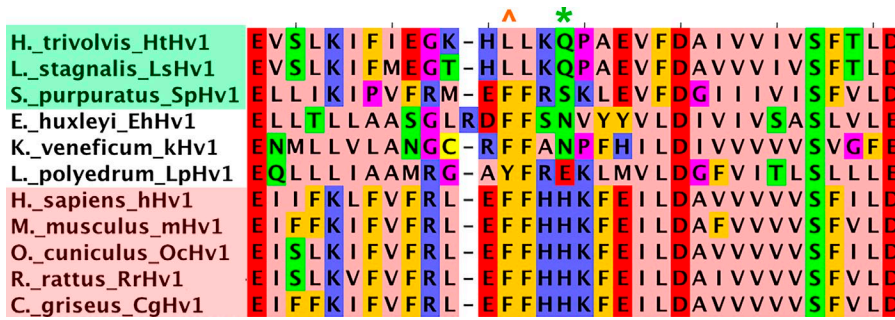


Figure 1. **Alignment of Hv1 S2-S3 linker and nearby regions (E153–D185 in hHv1).** Hv1 from several species were characterized as activating rapidly (green background: HtHv1, LsHv1, and SpHv1) or slowly (pink background: hHv1, mHv1, OcHv1, RrHv1, and CgHv1) based on available electrophysiological data. Unshaded species exhibit intermediate kinetics. In hHv1 numbering, the asterisk (*) indicates the position corresponding to the throttle histidine H168; the caret (^) indicates the position corresponding to F165. The S2-S3 linker in hHv1 encompasses K157–F165 (Li et al., 2015).

acid extrusion from cells (DeCoursey, 2003). Functions of Hv1 beyond acid extrusion, such as compensating electrically for the electrogenic activity of NADPH oxidase (Henderson et al., 1987; DeCoursey et al., 2003; DeCoursey, 2010), also require ΔpH dependent gating to enable Hv1 to open appropriately (Murphy and DeCoursey, 2006).

The phenomenon of ΔpH -dependent gating seems to be remarkably robust. Despite at least 171 different Hv1 mutants having been characterized electrophysiologically (DeCoursey et al., 2016), mutation at only one position, Trp²⁰⁷ (in hHv1 numbering), significantly altered ΔpH -dependent gating (Cherny et al., 2015). Mutation to this Trp resulted in premature saturation of the response to pH_o but did not affect pH_i responses. Recently identified Hv1 in a few species (Cherny et al., 2015; Chaves et al., 2016), including the voltage-gated proton channel gene in the snail *Helisoma trivolvis* (HtHv1; Thomas et al., in this issue), have an exaggerated pH_o response, shifting more than 40 mV/unit. Evaluation of three dozen hHv1 mutants revealed shifts of the absolute voltage dependence over a 270-mV range, but every mutant still exhibited an ~ 40 -mV/pH unit shift from whatever its starting voltage was (Ramsey et al., 2010). We were therefore surprised to find that despite a robust pH_o response, the WT HtHv1 channel has anomalously weak pH_i dependence, with the $g_{\text{H}}-V$ relationship shifting just 20 mV/unit or less (Thomas

et al., 2018). While testing several possible explanations for the rapid gating of snail HtHv1, we serendipitously discovered that replacement of a single amino acid, His¹⁶⁸, in the human channel nearly abolishes its pH_i dependence. We conclude that His¹⁶⁸ is a crucial component of pH_i sensing in hHv1.

Materials and methods

Electrophysiological and mutagenesis methods for HtHv1 are described in the accompanying article (Thomas et al., 2018); mutagenesis of hHv1 was described previously (Musset et al., 2010). A triple mutant of hHv1 (H167N/H168V/K168N) was supplied by I. Scott Ramsey and David E. Clapham (Harvard Medical School, Boston, MA). Statistical comparison of groups was done by using Student's *t* test.

Sequence analysis

46 full-length Hv1 sequences, including 11 electrophysiologically confirmed and 13 high-confidence sequences from protists—previously shown to be more diverse than animal Hv1 (Smith et al., 2011)—were aligned with MAFFT (Katoh and Standley, 2013). Sequences were trimmed to the voltage-sensing domain as described previously (Smith et al., 2011). Sequences that were not confirmed electrophysiologically were excluded, and empty

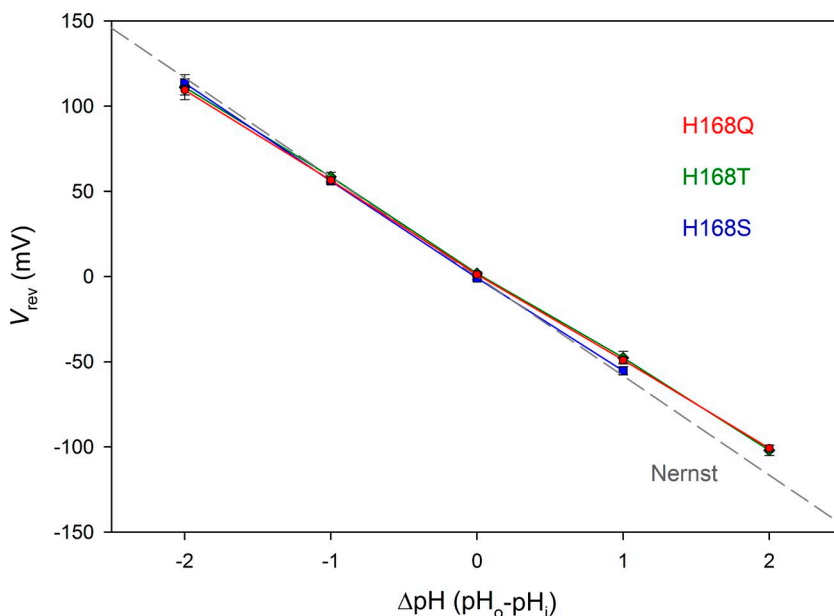


Figure 2. **His¹⁶⁸ mutants are proton selective.** Mean \pm SEM values for the reversal potential (V_{rev}) are plotted for 12 H168Q, 9 H168T, and 6 H168S cells or patches. The linear regression slope for each mutant is -52.6 , -53.2 , and -56.3 mV/unit change in ΔpH , respectively. For comparison, the gray dashed line shows the Nernst potential, E_{H} , expected for perfect H^+ selectivity.

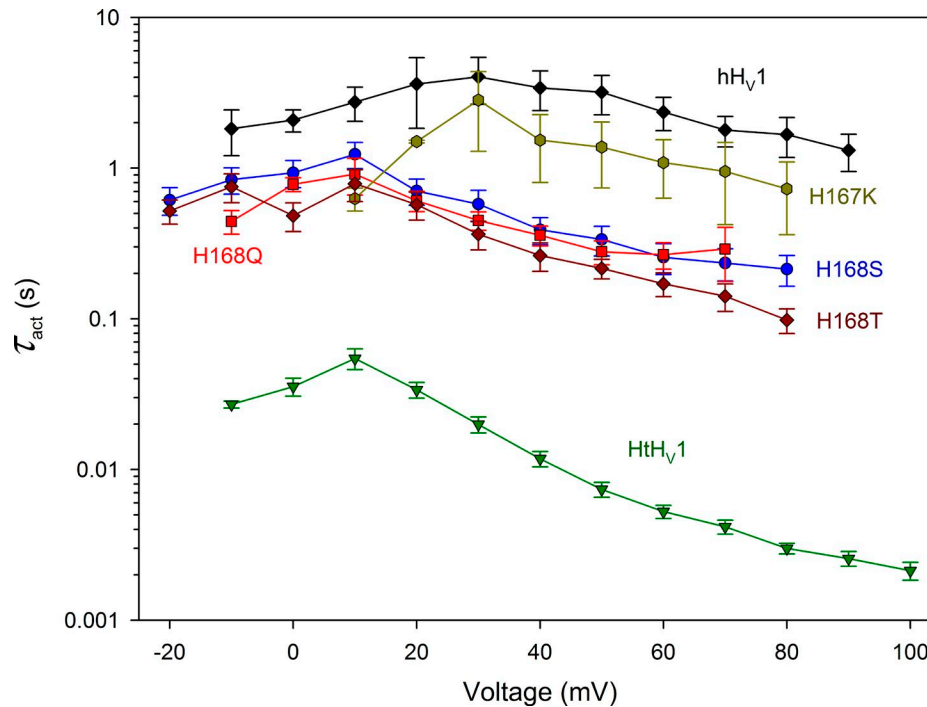


Figure 3. **The throttle histidine explains only a fraction of the rapid activation of HtHv1.** Activation time constants (τ_{act}) were determined by single exponential fits to currents in WT HtHv1, WT hHv1, and in four hHv1 mutants, as indicated, all at pH_o 7 and pH_i 7. Mean \pm SEM is plotted for 3–12 WT hHv1, 2–3 H167K, 3–6 H168S, 3–9 H168Q, 3–6 H168T, and 7–17 WT HtHv1. At all voltages from -10 to +80 mV, the WT hHv1 value is significantly larger than that of H168T, H168S, and H168Q combined and larger than HtHv1 ($P < 0.01$). The WT hHv1 data were taken from [Cherny et al. \(2015\)](#) and the HtHv1 data from [Thomas et al. \(2018\)](#).

columns removed from the alignment. The activation (opening) kinetics of electrophysiologically confirmed sequences were characterized as fast (*H. trivolvis*, HtHv1; *Lymnaea stagnalis*, LsHv1; and *Strongylocentrotus purpuratus*, SpHv1) or slow (*Homo sapiens*, hHv1; *Mus musculus*, mHv1; *Oryctolagus cuniculus*, OcHv1; *Rattus norvegicus*, RnHv1; and *Cricetulus griseus*, CgHv1); sequences with intermediate or unknown kinetics were removed. To identify sequence sites that distinguish sequence subfamilies, the alignment was submitted to the SPEER server ([Chakraborty et al., 2012](#)) with either user-defined (two subfamilies) or automated subgrouping and the following parameters: single-submission eight sequences, Relative Entropy term, PC Property Distance term, and Type. The same alignment but in randomized sequence order was also submitted with the automated subgrouping parameter and all other parameters as above. Sites corresponding to His¹⁶⁷ and His¹⁶⁸ in hHv1 were identified as appearing in the top 10 sites identified in all analyses and having a P value of <0.05 in at least one analysis.

Results

Is His¹⁶⁸ responsible for the slow gating kinetics of hHv1?

In our companion article ([Thomas et al., 2018](#)), we reported the identification of an Hv1 in a snail *H. trivolvis* (HtHv1) that exhibited rapid activation kinetics as reported for native proton currents in other snails ([Byerly et al., 1984](#)). We performed an analysis of subfamily determining sites to distinguish Hv1 sequences with fast versus slow gating kinetics. Species categorized as having fast gating included snails, HtHv1 ([Thomas et al.,](#)

[2018](#)) and *L. stagnalis*, LsHv1 ([Byerly et al., 1984](#)); and sea urchin, *S. purpuratus*, SpHv1 ([Sakata et al., 2016](#)) and are shaded green in [Fig. 1](#). Species with slow gating are human, hHv1 ([Bernheim et al., 1993](#); [DeCoursey and Cherny, 1993](#); [Demaurex et al., 1993](#)); mouse, mHv1 ([Kapus et al., 1993](#)); rabbit, *O. cuniculus*, OcHv1 ([Nordström et al., 1995](#)); rat, *R. norvegicus*, RnHv1 ([DeCoursey, 1991](#)); and Chinese hamster, *C. griseus*, CgHv1 ([Cherny et al., 1997](#)) and are shaded pink in [Fig. 1](#). This analysis pointed to two residues corresponding to His¹⁶⁷ and His¹⁶⁸ in hHv1 numbering; these residues are in the intracellular S2/S3 loop, extending into the S3 transmembrane helix. [Sakata et al. \(2016\)](#) found that substituting either Ser or Thr for His¹⁶⁴ in mHv1, which corresponds to His¹⁶⁸ in hHv1 ([Fig. 1](#), asterisk), accelerated activation kinetics by an order of magnitude, raising the possibility that His in this position governs activation kinetics, acting as a “throttle.” The same substitutions at the neighboring His¹⁶³ had no effect. For these reasons we focused our experiments on the S2/S3 loop area.

Similar to [Sakata et al. \(2016\)](#), we engineered mutations of His¹⁶⁸, replacing it with Ser (H168S) or Thr (H168T). Because activation of snail HtHv1 is distinctly faster than that of sea urchin SpHv1, we reasoned that replacing His¹⁶⁸ with Gln, which is at the corresponding position in HtHv1 (H168Q), should cause even faster kinetics. As a control, we replaced the neighboring His¹⁶⁷ in hHv1 with Lys (H167K), which occupies this position in HtHv1 ([Fig. 1](#)). Finally, we tested a triple mutant, in which three consecutive titratable amino acids (His¹⁶⁸ and its immediate neighbors) were all replaced by neutral residues (H167N/H168V/K169N). Robust proton selective currents were observed in all mutants. Results from H168S, H168T, and H168Q mutants

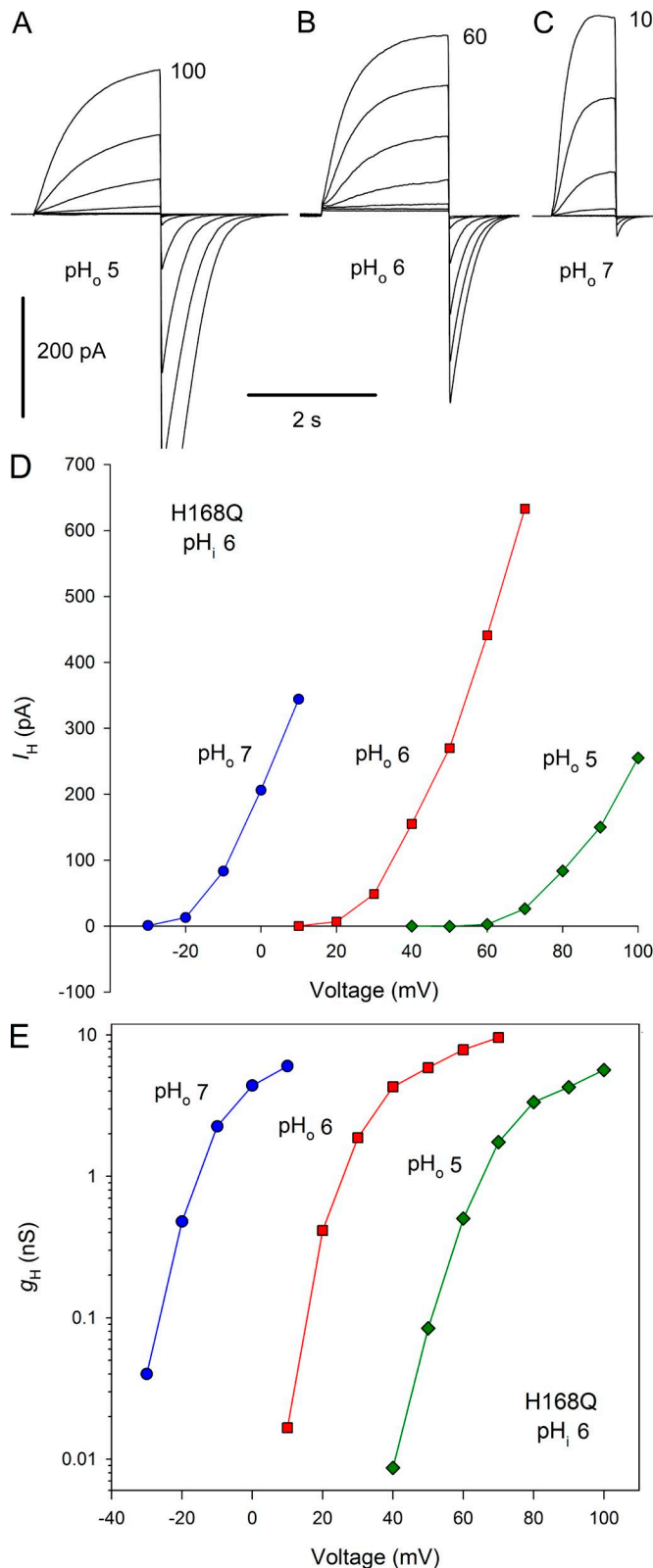


Figure 4. **Gating of His¹⁶⁸ mutants has normal pH_o dependence.** (A–C) Families of currents in a cell expressing the H168Q with pH_i 6 and pH_o 5, 6, and 7, with pulses in 10-mV increments up to the voltage indicated. Holding potential, V_{hold} was –40 mV (A and B) or –60 mV (C). (D and E) Proton current–voltage curves (D) and g_H–V relationships (E) from the families in A–C exhibit a normal 40-mV shift/unit change in pH_o.

were indistinguishable, and we thus refer to all such mutants as H168X. Fig. 2 shows that the reversal potential (V_{rev}) in the three H168X mutants was close to the Nernst potential, confirming proton selectivity.

Fig. 3 illustrates the effects of these mutations on channel-opening kinetics. Replacing His¹⁶⁸ with any of the three amino acids (Ser, Thr, or Gln) produced a 10-fold speeding of the activation (opening) time constant (τ_{act}) in the positive voltage range, much like the analogous effect in mHv1 (Sakata et al., 2016). Mutating the neighboring His¹⁶⁷ had no clear effect. That the effects of the three substituents (Ser, Thr, or Gln) were identical suggests that the speeding of activation is caused by removing the imidazole group of His and is not caused by introducing other side chains at this position. Thus, the hydroxyl group of Thr or Ser was no more or less effective than the amide group of Gln. Presumably, His¹⁶⁸ interacts specifically with other parts of the hHv1 channel in a manner that results in slower activation. Nevertheless, despite the distinct acceleration caused by His¹⁶⁸ removal, τ_{act} remained much slower than in the WT snail channel HtHv1.

His¹⁶⁸ mutation alters ΔpH-dependent gating of hHv1

The His¹⁶⁸ mutants exhibited normal responses to changes in pH_o. Families of currents in a cell expressing the H168Q mutant are shown in Fig. 4, A–C. The currents appear qualitatively like WT hHv1 currents, although with somewhat faster activation. Changing pH_o from 5 to 6 to 7 shifted the H⁺ current (I_H)–V (Fig. 4 D) and g_H–V relationships (Fig. 4 E) by ~40 mV/unit. This behavior conforms to the classical “rule of forty” observed for Hv1 in all species thus far examined (DeCoursey, 2013), except for HtHv1 as described in the companion article (Thomas et al., 2018).

In contrast, mutation of His¹⁶⁸ to Ser, Thr, or Gln greatly weakened the sensitivity of the mutant channels to pH_i. Fig. 5, A–E shows currents in an inside-out patch with H168T at pH_o 7 and pH_i ranging from 5 to 9. Although the I_H–V relationship does shift positively at higher pH_i (Fig. 5 F), the shift is distinctly <40 mV, especially at high pH_i, with the result that there are inward currents over a wide voltage range. Inward currents in WT hHv1 are rarely observed and occur mainly with large outward pH gradients (Musset et al., 2008). It is evident from the g_H–V relationships (Fig. 5 G) that the shifts are ≤20 mV/unit over the entire pH_i range studied.

Measurements of the position of the g_H–V relationship in several cells and patches are summarized in Fig. 6 A, quantified as V(g_{H,max}/10), the voltage at which g_H reached 10% of g_{H,max}, its maximal value. Changes in pH_o for the H168X mutants (Fig. 6 A, blue circles) produce a slope of 40 mV/unit up to pH_o 8 (ΔpH = 1). This behavior is identical to the WT hHv1 response (Cherny et al., 2015). Data from inside-out patches (Fig. 6 A, dark red diamonds) reveal that the H168X mutants exhibit a greatly attenuated pH_i response. The entire curve has a mean slope of only 16.1 mV/unit. However, the relationship appears steeper at high ΔpH. Omitting the point at ΔpH = 2 (pH_o 7, pH_i 5), the mean slope drops to 12.6 mV/unit.

The behavior of the H168X mutants strikingly resembles that of WT HtHv1, as illustrated in Fig. 6 B. The data for HtHv1 from the companion article (Thomas et al., 2018) are replotted here (Fig. 6 B, open symbols and dotted lines) for comparison.

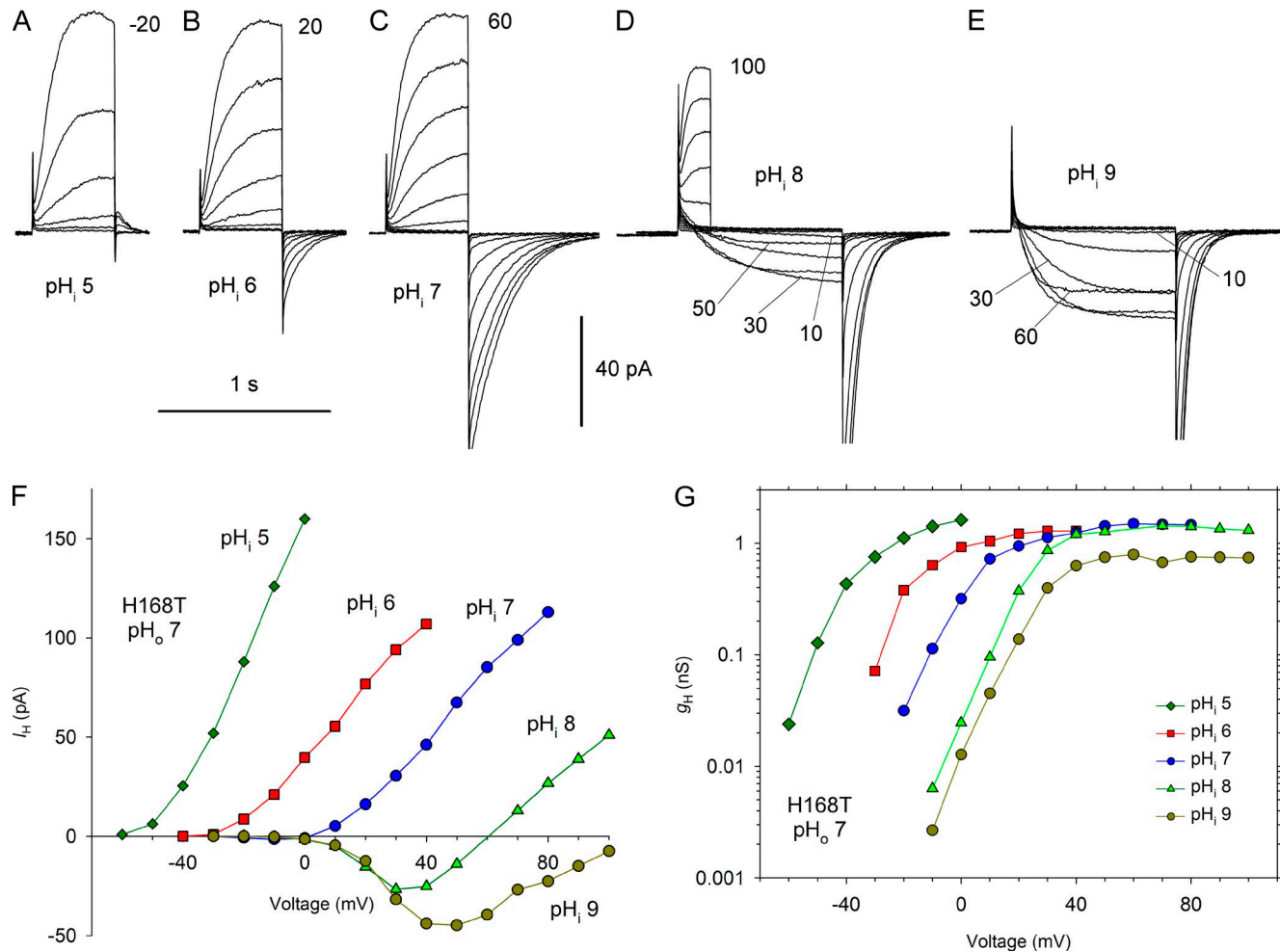


Figure 5. Mutation of His¹⁶⁸ in hHv1 weakens the pH_i dependence of gating. (A–E) Families of currents at several pH_i values in an inside-out patch from a cell transfected with H168T, with pH_o 7 in the pipette. Pulses were applied in 10-mV increments up to the voltage indicated from V_{hold} = –80 mV (A), –60 mV (B), or –40 mV (C–E). (D) Shorter pulses were applied to 60 mV and above, and the tail currents have been removed. (E) Pulses above 60 mV were omitted for clarity. (F) Current–voltage curves. (G) g_H–V relationships from this experiment.

Comparison of pH_o responses reveals that HtHv1 has an exceptionally steep ΔpH dependence at pH_o 7 or less, roughly 60 mV/unit. The response to pH_o for H168X mutants (Fig. 6 B, shaded blue circles) is a 40-mV/unit shift, which is normal for human hHv1 (Cherny et al., 2015). The response of H168X mutants to pH_i changes (Fig. 6 B, red diamonds) is notably weak and closely parallels the response of WT snail HtHv1. With respect to ΔpH-dependent gating, the mutation of a single amino acid, His¹⁶⁸, effectively converts the human channel into a snail channel.

The immediate neighbors of His¹⁶⁸ do not appear to contribute

Located next the His¹⁶⁸ that plays a critical role in pH_i sensing is another His, His¹⁶⁷. We wondered whether this nearby position might share the effect. However, the single mutation H167K did not impair pH_i sensing. This specific replacement was selected because HtHv1 has Lys at the corresponding position (Fig. 1). Fig. 7 illustrates H⁺ currents in an inside-out patch expressing the H167K mutant at pH_i 6, 7, and 8. The g_H–V relationship shifted normally (Fig. 7 E). Mean data from three patches with H167K are plotted in Fig. 8, which shows that the pH_i response of this mutant is indistinguishable from that of WT hHv1. Furthermore,

Fig. 3 showed that the H167K mutation did not alter activation kinetics. Evidently, His¹⁶⁸ but not His¹⁶⁷ is located precisely where it can strongly influence gating in response to pH_i.

We also tested a triple mutant, in which three consecutive titratable amino acids at the inner end of the S3 helix were replaced by neutral residues (H167N/H168V/K169N). In inside-out patches with pH_o 7.5, studied at pH_i 5.5, 6.5, 7.5, and 8.5, the sensitivity to pH_i was weak, like that of the H168X single mutants. The mean slope by linear regression of the relationship between ΔpH and V(g_{H,max}/10) in seven patches was 20.1 mV/unit, similar to 16.1 mV/unit in H168X (Fig. 6), suggesting that the amino acids neighboring His¹⁶⁸ were inactive. This triple mutant was examined previously, and normal ΔpH dependence was reported (Ramsey et al., 2010). However, in that study only pH_o was varied, not pH_i. The triple mutant, like all single His¹⁶⁸ mutants, exhibits normal pH_o dependence but abnormally weak pH_i dependence.

Possible interaction between H168 and F165

Data on pH_i sensitivity are somewhat less abundant than for pH_o sensitivity, and much is derived from native tissues. Species with Hv1 that have been shown to exhibit classical rule of forty

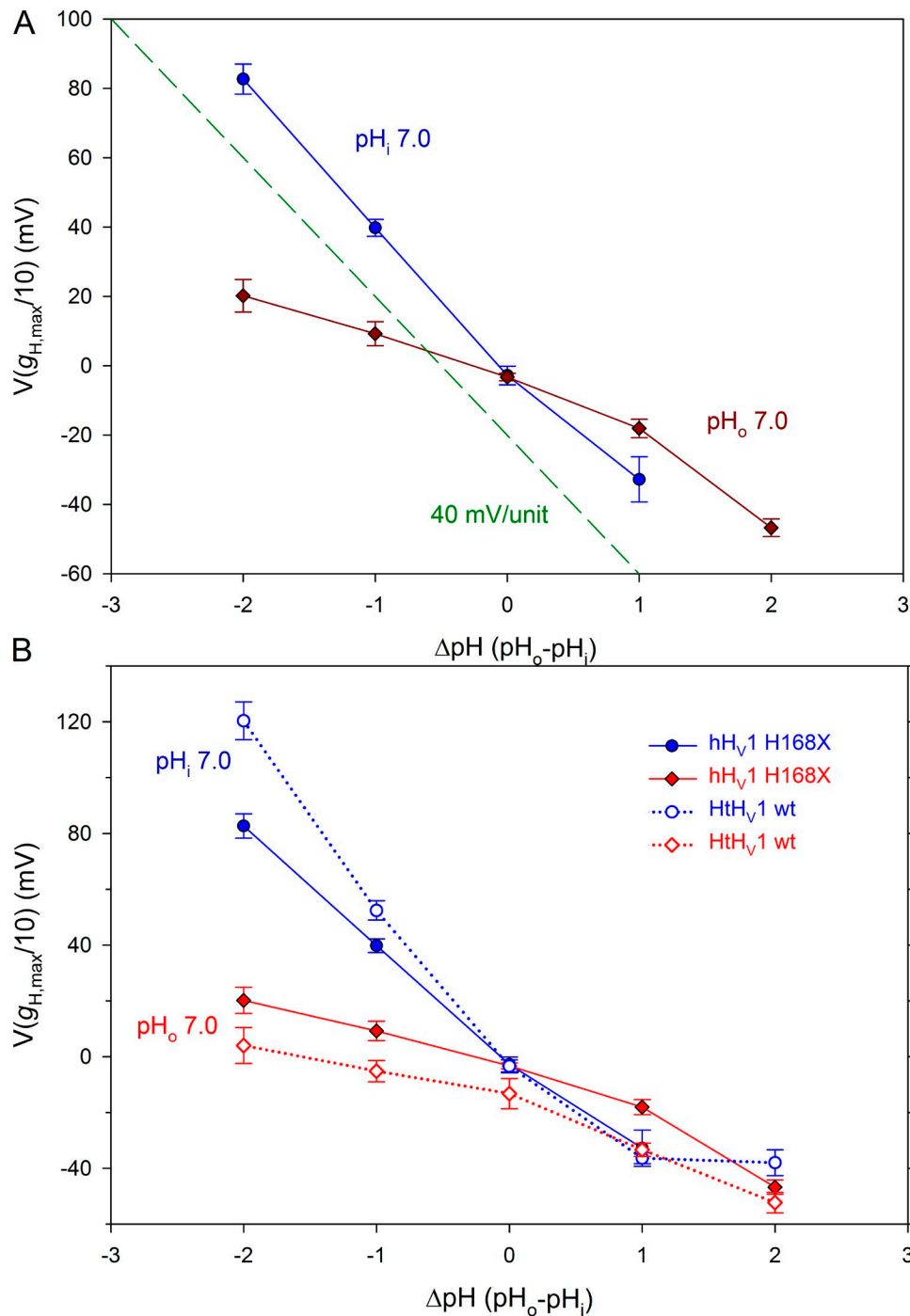


Figure 6. **The His¹⁶⁸ mutation recapitulates the anomalous ΔpH dependence of HtHv1.** (A) The effect of pH_o and pH_i on the position of the $g_{\text{H}}-V$ relationship in the three H168x mutants combined (mean \pm SEM) is plotted. The position of the $g_{\text{H}}-V$ relationship was defined in terms of $V(g_{\text{H,max}}/10)$. The dashed green line shows a slope of 40 mV/unit for reference. The dependence of these mutants on pH_o is normal, whereas their pH_i response is greatly attenuated. Linear regression on all points (ignoring the obvious nonlinearity) gives a slope of 38.9 mV/unit change in pH_o and 16.1 mV/unit change in pH_i . (B) The same data are replotted (shaded symbols) along with the analogous measurements for HtHv1 (open symbols) taken from Fig. 9 of the companion article (Thomas et al., 2018). In whole-cell measurements, pH_o was varied with pH_i 7 (blue symbols). When pH_i was varied by using inside-out patches with pH_o 7, there was very little shift of the $g_{\text{H}}-V$ relationship (red symbols). Numbers of cells for increasing ΔpH in H168X mutants for pH_i 7 are 3, 10, 11, and 5 and for pH_o 7 are 6, 10, 14, 11, and 4.

behavior for changes in pH_i include human (Demaurex et al., 1993; Gordienko et al., 1996; Schrenzel et al., 1996; Schilling et al., 2002), mouse (Kapus et al., 1993; Szteyn et al., 2012), *Rana pipiens* (Gu and Sackin, 1995), rat (Cherny et al., 1995; DeCoursey and Cherny, 1995), *Karlodinium veneficum* (Cherny et al., 2015),

Emiliana huxleyi (Cherny et al., 2015), and *Lingulodinium polyedrum* (Rodriguez et al., 2017). The only violators of the rule thus far are the snails *H. trivolvis* (Thomas et al., 2018) and *L. stagnalis* (Byerly et al., 1984). Another intriguing exception is a short isoform of hHv1 expressed in sperm that lacks the first 68 amino

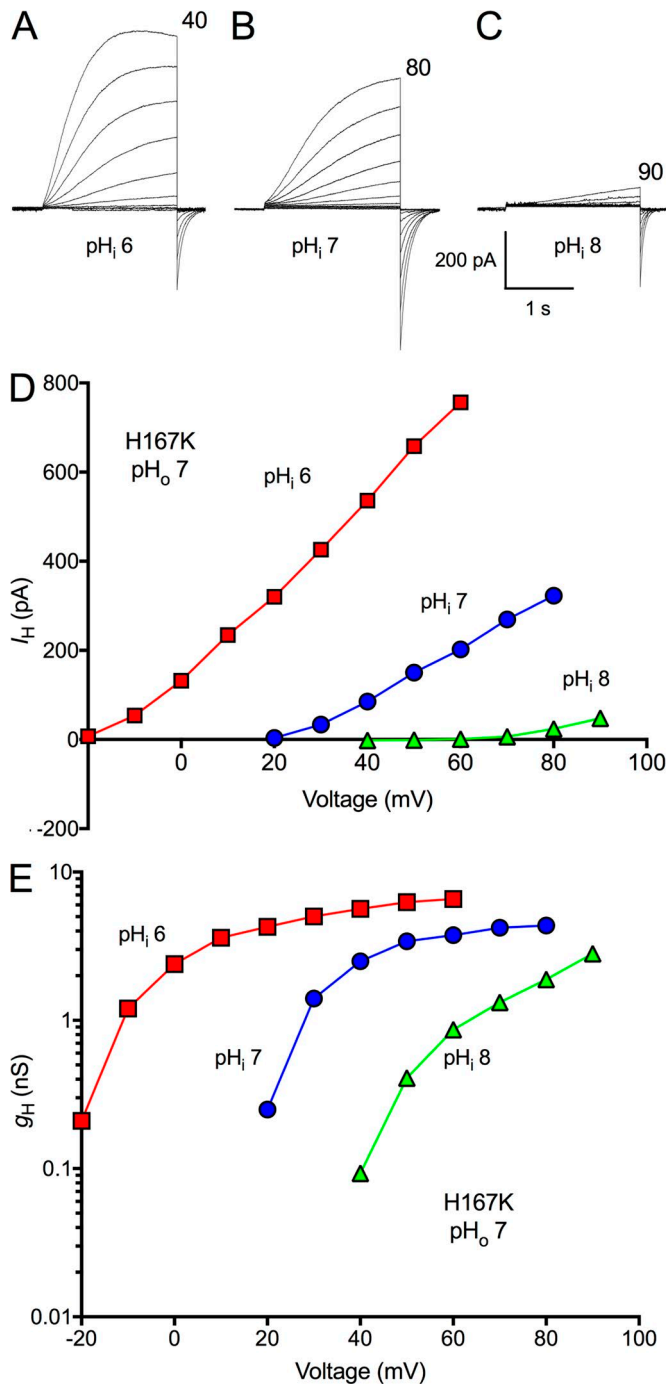


Figure 7. The H167K mutant of hHv1 has normal pH_i dependence. (A–C) Families of currents are shown in an inside-out patch with pH_o 7 and pH_i 6, 7, or 8, as labeled. Pulses were applied in 10-mV increments up to the voltage indicated, from V_{hold} = -60 mV (A) or -40 mV (B and C). (D and E) Current–voltage curves (D) and g_H–V relationships from this patch are illustrated (E). At pH_i 8, g_H was estimated from tail current amplitudes and scaled according to g_H calculated from the outward current at 90 mV.

acids of the N terminus and has weakened pH_i sensing (Berger et al., 2017). Inspection of sequences (Fig. 1) for which pH_i sensitivity has been measured directly (HtHv1, LsHv1, EhHv1, kHv1, LpHv1, hHv1, mHv1, and RnHv1) shows that Leu substitutes for Phe at the Phe¹⁶⁵ position (human numbering) in two species with rapid gating and attenuated pH_i responses, HtHv1 and LsHv1.

Although in the available crystal structure of Hv1 (Takeshita et al., 2014) this area did not have sufficient electron density to be visualized, molecular models of Hv1 (Kulleperuma et al., 2013; Li et al., 2015) indicate that Phe¹⁶⁵ could plausibly interact with the nearby His¹⁶⁸ through π -stacking or cation- π interactions.

To test the idea that His¹⁶⁸ interacts with Phe¹⁶⁵, we individually mutated Phe¹⁶⁵ and as a control, Phe¹⁶⁶. F166L produced robust currents, and as shown in Fig. 8, pH_i sensing of F166L was essentially normal and similar to that of WT hHv1. F165H and F165A (Fig. 8, F165X) produced currents that activated in a more negative voltage range than WT. To enable comparison of the slopes, 13.8 mV has been added to these data, so they superimpose on WT at Δ pH = 1. The pH_i sensitivity of F165A and F165H was closer to WT than to that of the H168X mutants. Finally, the double mutant F165L/H168Q was also close to the single H168X mutant data (unpublished data). Although these results do not rule out the possibility of interaction between His¹⁶⁸ and Phe¹⁶⁵, it appears that His¹⁶⁸ is distinctly more critical for pH_i sensing.

The converse mutation Q229H fails to impart human characteristics to the *H. trivolvis* channel

The single point mutation H168X (X = T, S, Q) profoundly alters the gating and pH sensing of the human channel hHv1, accelerating activation 10-fold and greatly attenuating the pH_i response. We next considered whether the converse mutation (Q229H) would impart humanoid characteristics to HtHv1. In short, this mutation had no discernable effect on the gating kinetics or pH sensitivity of HtHv1 (Fig. 9). The Q229H mutation did not slow activation; at +40 mV at pH_o 7, τ_{act} was 11.8 ± 1.4 ms ($n = 17$) in WT HtHv1 (Fig. 3) and 10.0 ± 2.0 ms ($n = 8$) in Q229H ($P = 0.53$). We assessed pH_o sensitivity in whole-cell experiments. Like WT HtHv1, activation kinetics was extremely sensitive to pH_o, whereas the deactivation or tail current (closing) time constant appeared to be pH_o independent. Like WT, changes in pH_o produced supernormal shifts in the position of the g_H–V relationship, averaging 57 mV/unit between pH_o 5 and 7 (Fig. 10), paralleling the WT response although the absolute voltages appear somewhat more negative. Similarly, the Q229H mutation did not discernibly change the weak response of HtHv1 to changes in pH_i (Figs. 9 E and 10). In three inside-out patches studied at pH_i 5, 6, 7, and 8, the slope of the mean dependence of V(g_{H,max}/10) on Δ pH was 18 mV/unit by linear regression. It is clear that the extraordinary changes to the pH_i response of the human channel resulting from His¹⁶⁸ mutation reflect interactions that are not confined to this single amino acid and therefore are not easily transferred.

Discussion

Is the human hHv1 channel slow because of the throttle residue, His¹⁶⁸?

The sea urchin proton channel, SpHv1, exhibits rapid activation kinetics 20–60 times faster than the mouse mHv1. Sakata et al. (2016) investigated the structural basis for this property and, by creating progressively smaller chimeras with mHv1, finally identified a single amino acid (Ser) at the inner end of the S3 transmembrane segment that appeared largely responsible. Introducing Ser into mHv1 (H164S) accelerated mouse activation kinetics

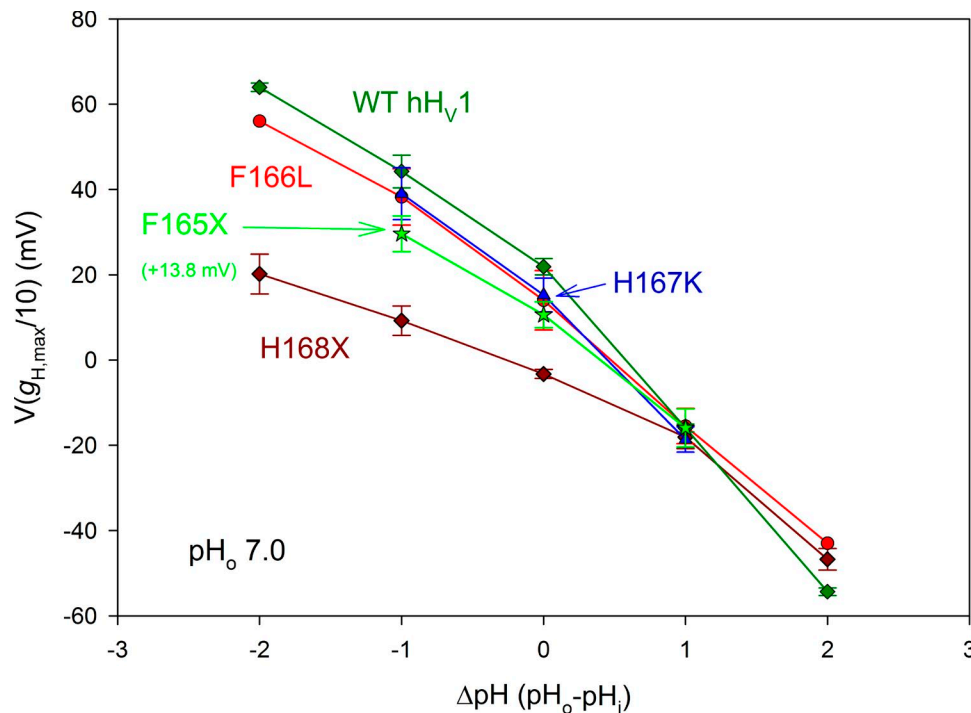


Figure 8. **The F166L and H167K mutations do not impair pH_i sensing of hHv1.** The pH_i responses of the H168X mutants are replotted from Fig. 6. The pH_i responses of WT hHv1, the F166L mutant of hHv1, and the H167K mutant of hHv1 are indistinguishable from each other. The F165X data are from three F165A and three F165H patches combined, and 13.8 mV has been added to all values to facilitate comparison with WT. All data (mean \pm SEM) come from inside-out patches studied at pH_o 7, with $n = 2-9$ (H168X), 1-4 (F166L), 3 (H167K), and 6 (F165X).

by more than an order of magnitude. In mHv1, H164T produced speeding similar to H164S, suggesting that the hydroxyl group is important (Sakata et al., 2016). Intriguingly, however, the converse mutation, and even substituting the entire S3 helix from mHv1 into SpHv1, failed to slow the kinetics of the latter.

We engineered mutations of human hHv1 at His¹⁶⁸ (the position that corresponds to His¹⁶⁴ in mHv1), replacing the His with Ser (H168S), Thr (H168T), or Gln (H168Q). In most respects, the results resembled those in mHv1: mutations at His¹⁶⁸ accelerated activation by about one order of magnitude (Fig. 3). Because HtHv1 has Gln at the corresponding position and HtHv1 is distinctly faster than SpHv1, we expected that Gln substitution might produce faster activation; however, activation kinetics of H168Q were very similar to those of H168S and H168T, all of which remained much slower than that of WT HtHv1 (Fig. 3). Because the three mutants behaved indistinguishably, we conclude that the effects result from the removal of the imidazole side chain of His¹⁶⁸ and not from the side chains that replace it.

The precise location of His¹⁶⁸ is important. The His immediately adjacent to His¹⁶⁸ does not share its impact on gating kinetics. Sakata et al. (2016) replaced His¹⁶³ in mHv1 with the SpHv1 residue at the corresponding position (H163R); this mutation had little effect on kinetics of mHv1. We replaced His¹⁶⁷ in hHv1 with Lys, which occupies the corresponding position in HtHv1. In neither species was activation kinetics appreciably affected (Fig. 3).

Also, similar to the results in mHv1, the converse mutation substituting the hHv1 residue for the HtHv1 throttle residue, Q229H, did not slow HtHv1 kinetics. Therefore, the mechanism by which His¹⁶⁸ retards activation must require interaction with

other parts of the protein that are absent in Hv1 from species with rapid gating.

His¹⁶⁸ in hHv1 is crucial for pH_i sensing

In searching for a mechanistic explanation for the rapid gating kinetics of HtHv1, we serendipitously identified a histidine near the inner end of the channel that is crucial for pH_i sensing. Transferring the Gln²²⁹ from the snail channel HtHv1 to replace His¹⁶⁸ in the human channel hHv1 (Fig. 1) reproduced the impoverished pH_i sensing of HtHv1 almost exactly (Fig. 6B). Because three different substituents (Ser, Thr, and Gln) had indistinguishable effects (Figs. 3 and 6), it appears that a specific property of His in this position is involved. Because the converse mutation (Q229H) did not transfer human-like pH_i sensing (or activation kinetics) to HtHv1 (Fig. 9), His¹⁶⁸ must perform pH_i sensing by interacting with its immediate environment in the human channel. This conclusion is reinforced by the fact that three unicellular species that lack His at this position (kHv1, LpHv1, and EhHv1; Fig. 1) exhibit normal pH_i sensitivity (Cherny et al., 2015; Rodriguez et al., 2017). Replacing the neighboring His¹⁶⁷ had no effect, and mutating both His¹⁶⁷ and Lys¹⁶⁹ (HHK→NVN) had no effect beyond that of His¹⁶⁸ alone, indicating that the specific location at position 168 is critical.

When the ΔpH dependence of Hv1 gating was discovered (Cherny et al., 1995), the simplest model that could reproduce the entire phenomenon postulated a single pH sensor with alternating access to both internal and external solutions. An expanded model with additional complexity includes distinct external and internal pH sensors. A “counter-charge” model has been suggested in which protonation disrupts charge-pair interactions,

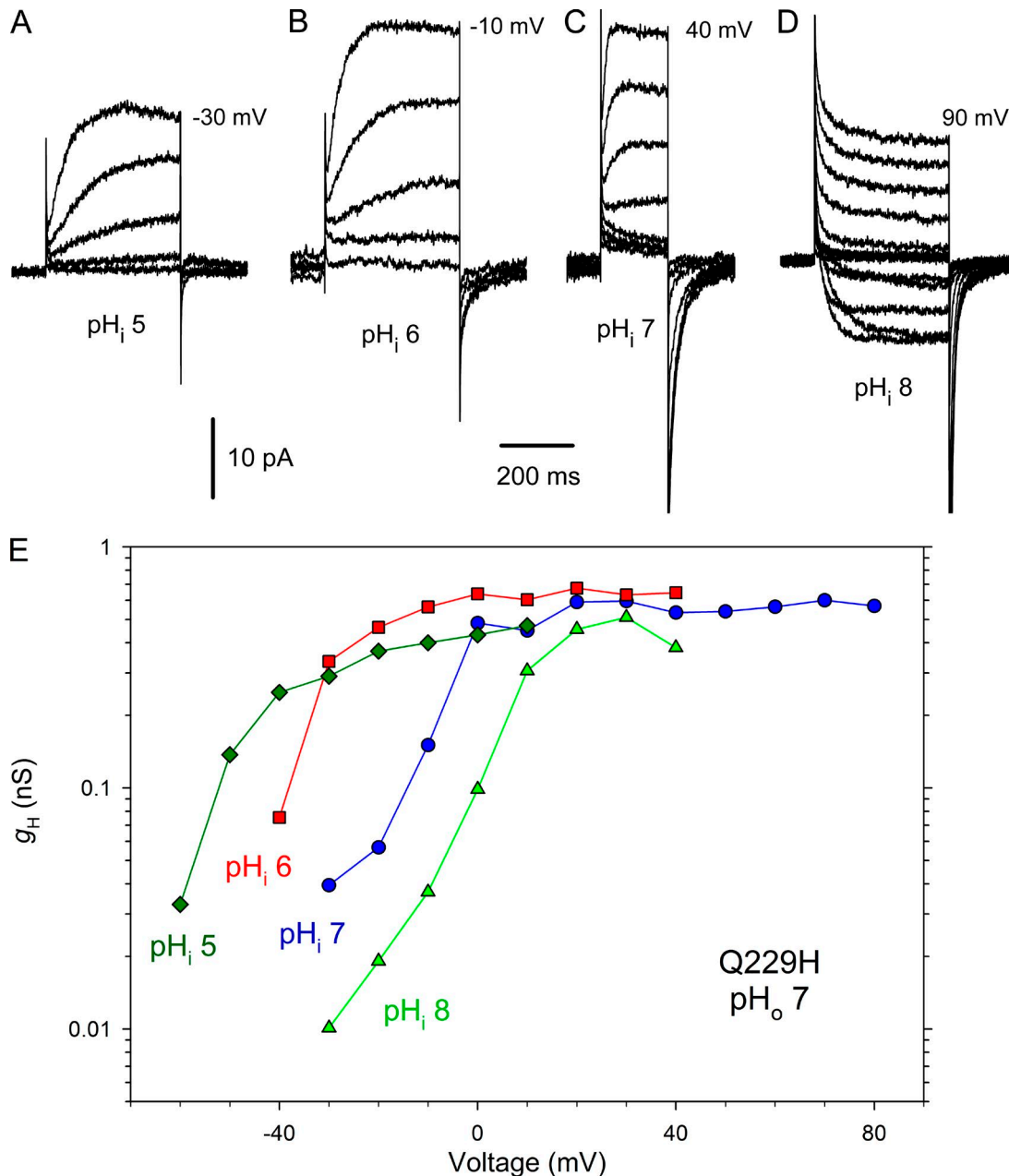


Figure 9. **The Q229H mutation does not restore human-like activation kinetics or pH_i sensitivity to HtHv1.** (A–D) Families of currents in an inside-out patch with pH_o 7 in the pipette solution in 10-mV increments up to the voltage shown from $V_{hold} = -80, -60, -40,$ and -40 mV, at pH_i 5, 6, 7, and 8, respectively. (E) Currents from this patch converted to g_H produce g_H - V relationships that shift much less than 40 mV/unit. Corresponding measurements in WT HtHv1 are plotted in Fig. 5 G.

so that low pH_i promotes opening and low pH_o promotes closing (DeCoursey, 2018). A different kind of proposal for pH sensing does not invoke titratable pH sensors; instead, protonated waters in Hv1 communicate information about local pH through electrostatic interactions with the voltage-sensing Arg residues in the S4 helix (Ramsey et al., 2010). Recently, the first mutation in Hv1 documented to compromise pH sensing was reported (Cherny et al., 2015). In these Trp mutants, pH_o but not pH_i sensitivity was affected, suggesting that separate pH_o and pH_i sensors exist in Hv1. Intriguingly, like the H168X mutants, these W207X mutants also dramatically accelerated hHv1 gating kinetics, and HtHv1 itself has extremely rapid gating.

That HtHv1 has normal pH_o sensitivity but anemic pH_i sensitivity suggests that its ΔpH dependence is accomplished by distinct external and internal pH sensors. That the H168x mutation in hHv1 selectively attenuates its pH_i sensitivity without affecting its pH_o sensitivity further supports the existence of distinct external and internal pH sensors.

To search for a structural basis for this species difference in pH_i sensing, we compared the sequences of Hv1 in species in which pH_i responses have been documented to obey the rule of forty (human, mouse, rat, *K. veneficum*, *E. huxleyi*, and *L. polyedrum*; excepting *R. pipiens* for which we could find no sequence), to the sequence of HtHv1 with its anomalously weak

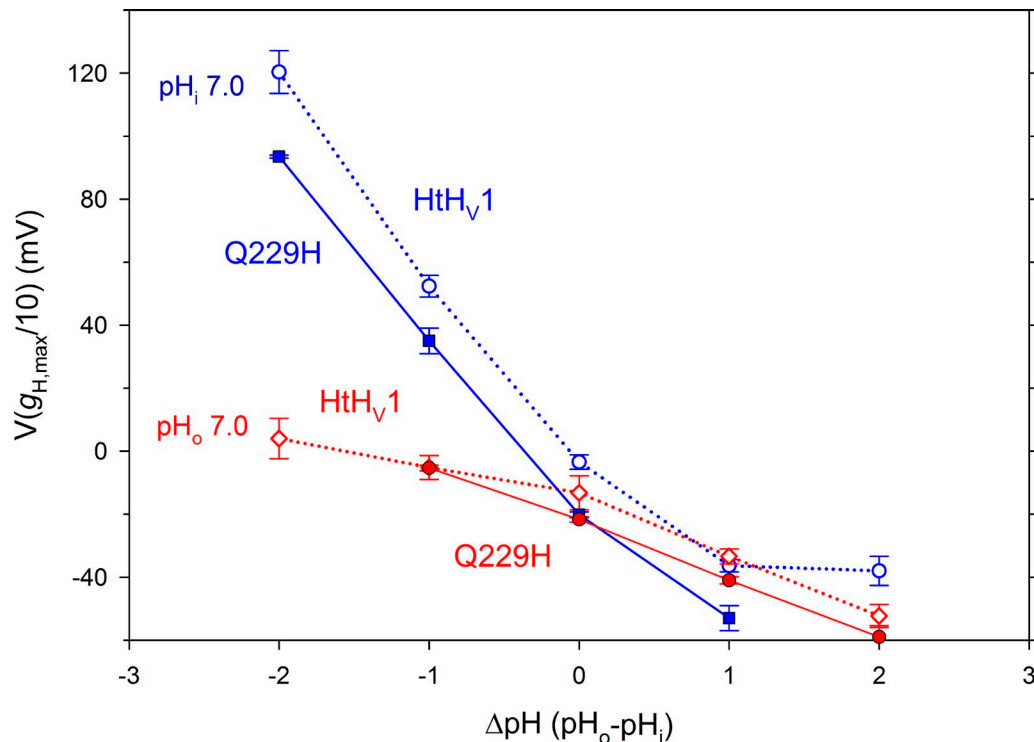


Figure 10. **The Q229H mutation does not restore human-like pH_i sensitivity to HtH_v1.** The dependence of the position of the g_H - V relationship on both pH_o and pH_i is similar in WT HtH_v1 (open symbols and dotted lines) and in the Q229H mutant (shaded symbols and solid lines). The WT data are replotted from Fig. 6 B. Mean \pm SEM are shown for $n = 2$ –5 cells with pH_i 7 and three inside-out patches with pH_o 7.

sensitivity to pH_i. We noticed a striking substitution in HtH_v1, in which Phe¹⁶⁵ (human numbering; Fig. 1) is replaced by Leu. This position is very highly conserved: in the alignment of 46 H_v1 sequences that includes vertebrates, invertebrates, and protists, Phe is replaced by the conservative Tyr five times, by Leu twice, and by Met once. In this context, it is important to note that the protist H_v1 sequences are more diverse than all animal sequences (Smith et al., 2011), highlighting the very high conservation of Phe at this position. The two snail species in which Leu replaces Phe (HtH_v1 and LsH_v1) both have rapid gating and weak pH_i sensitivity (Fig. 1). In structural models of H_v1 (Kulleperuma et al., 2013; Li et al., 2015), Phe¹⁶⁵ is in a position in which it could plausibly interact with His¹⁶⁸, through π -stacking or cation- π interactions. Reasoning that such an interaction might be part of the pH_i-sensing mechanism, we replaced Phe¹⁶⁵ in hH_v1 with Ala or His to attempt to disrupt the interaction. Both F165A and F165H exhibited pH_i sensing intermediate between WT and the H168x mutants but closer to WT hH_v1. The neighboring F166L mutation did not affect pH_i sensing (Fig. 8). For geometrical reasons, we consider it more likely that His¹⁶⁸ could interact with Phe¹⁶⁵ than with Phe¹⁶⁶ because the latter would be constrained by proximity. Intrahelical $i, i + 2$ side-chain-side-chain contacts are statistically improbable (Walther and Argos, 1996). That Phe¹⁶⁵ mutants were activated at more negative voltages than WT (Fig. 8) is consistent with F165-H168 interaction impeding hH_v1 opening. That the insertion of His into the corresponding position in HtH_v1 did not enhance pH_i sensitivity indicates that the mere presence of His at this location is not sufficient, but that to affect pH_i sensing requires additional interaction. Evidently, and perhaps

surprisingly, the intracellular S2-S3 linker is of central importance in sensing pH_i in human hH_v1. Furthermore, the selective effect of mutations in this region on pH_i sensing while leaving pH_o sensing intact supports the idea that Δ pH-dependent gating of H_v1 relies on independent internal and external pH sensors.

Acknowledgments

This work was supported by National Institutes of Health grants GM102336 (to T.E. DeCoursey and S.M.E. Smith) and GM121462 (to T.E. DeCoursey) and National Science Foundation grant MCB-1242985 (to T.E. DeCoursey and S.M.E. Smith).

The authors declare no competing financial interests.

Author contributions: S.M.E. Smith and T.E. DeCoursey conceptualized the study. T.E. DeCoursey curated the data. S. Thomas, S.M.E. Smith, V.V. Cherny, D. Morgan, and T.E. DeCoursey performed the formal analysis. T.E. DeCoursey and S.M.E. Smith acquired the funding. V.V. Cherny and D. Morgan performed the investigation. S.M.E. Smith and T.E. DeCoursey administered the project. S. Thomas and S.M.E. Smith provided the resources. S.M.E. Smith and T.E. DeCoursey visualized the study. T.E. DeCoursey wrote the original draft of the manuscript. S.M.E. Smith and T.E. DeCoursey reviewed and edited the manuscript.

Richard W. Aldrich served as editor.

Submitted: 7 December 2017

Accepted: 27 March 2018

References

- Bennett, A.L., and I.S. Ramsey. 2017. CrossTalk opposing view: proton transfer in Hv1 utilizes a water wire, and does not require transient protonation of a conserved aspartate in the S1 transmembrane helix. *J. Physiol.* 595:6797–6799. <https://doi.org/10.1113/JP274553>
- Berger, T.K., D.M. Fußh oller, N. Goodwin, W. B onigk, A. M uller, N. Dokani Khesroshahi, C. Brenker, D. Wachten, E. Krause, U.B. Kaupp, and T. Str unker. 2017. Post-translational cleavage of Hv1 in human sperm tunes pH- and voltage-dependent gating. *J. Physiol.* 595:1533–1546. <https://doi.org/10.1113/JP273189>
- Bernheim, L., R.M. Krause, A. Baroffio, M. Hamann, A. Kaelin, and C.R. Bader. 1993. A voltage-dependent proton current in cultured human skeletal muscle myotubes. *J. Physiol.* 470:313–333. <https://doi.org/10.1113/jphysiol.1993.sp019860>
- Byerly, L., R. Meech, and W. Moody Jr. 1984. Rapidly activating hydrogen ion currents in perfused neurones of the snail, *Lymnaea stagnalis*. *J. Physiol.* 351:199–216. <https://doi.org/10.1113/jphysiol.1984.sp015241>
- Chakraborty, A., S. Mandloi, C.J. Lanczycki, A.R. Panchenko, and S. Chakrabarti. 2012. SPEER-SERVER: a web server for prediction of protein specificity determining sites. *Nucleic Acids Res.* W242–W248. <https://doi.org/10.1093/nar/gks559>
- Chamberlin, A., F. Qiu, S. Rebollo, Y. Wang, S.Y. Noskov, and H.P. Larsson. 2014. Hydrophobic plug functions as a gate in voltage-gated proton channels. *Proc. Natl. Acad. Sci. USA.* 111:E273–E282. <https://doi.org/10.1073/pnas.1318018111>
- Chaves, G., C. Derst, A. Franzen, Y. Mashimo, R. Machida, and B. Musset. 2016. Identification of an Hv1 voltage-gated proton channel in insects. *FEBS J.* 283:1453–1464. <https://doi.org/10.1111/febs.13680>
- Cherny, V.V., and T.E. DeCoursey. 1999. pH-dependent inhibition of voltage-gated H⁺ currents in rat alveolar epithelial cells by Zn²⁺ and other divalent cations. *J. Gen. Physiol.* 114:819–838. <https://doi.org/10.1085/jgp.114.6.819>
- Cherny, V.V., V.S. Markin, and T.E. DeCoursey. 1995. The voltage-activated hydrogen ion conductance in rat alveolar epithelial cells is determined by the pH gradient. *J. Gen. Physiol.* 105:861–896. <https://doi.org/10.1085/jgp.105.6.861>
- Cherny, V.V., L.M. Henderson, and T.E. DeCoursey. 1997. Proton and chloride currents in Chinese hamster ovary cells. *Membr. Cell Biol.* 11:337–347.
- Cherny, V.V., R. Murphy, V. Sokolov, R.A. Levis, and T.E. DeCoursey. 2003. Properties of single voltage-gated proton channels in human eosinophils estimated by noise analysis and by direct measurement. *J. Gen. Physiol.* 121:615–628. <https://doi.org/10.1085/jgp.200308813>
- Cherny, V.V., D. Morgan, B. Musset, G. Chaves, S.M.E. Smith, and T.E. DeCoursey. 2015. Tryptophan 207 is crucial to the unique properties of the human voltage-gated proton channel, hHv1. *J. Gen. Physiol.* 146:343–356. <https://doi.org/10.1085/jgp.201511456>
- DeCoursey, T.E. 1991. Hydrogen ion currents in rat alveolar epithelial cells. *Biophys. J.* 60:1243–1253. [https://doi.org/10.1016/S0006-3495\(91\)82158-0](https://doi.org/10.1016/S0006-3495(91)82158-0)
- DeCoursey, T.E. 2003. Voltage-gated proton channels and other proton transfer pathways. *Physiol. Rev.* 83:475–579. <https://doi.org/10.1152/physrev.00028.2002>
- DeCoursey, T.E. 2010. Voltage-gated proton channels find their dream job managing the respiratory burst in phagocytes. *Physiology (Bethesda)*. 25:27–40. <https://doi.org/10.1152/physiol.00039.2009>
- DeCoursey, T.E. 2013. Voltage-gated proton channels: molecular biology, physiology, and pathophysiology of the H_v family. *Physiol. Rev.* 93:599–652. <https://doi.org/10.1152/physrev.00011.2012>
- DeCoursey, T.E. 2015. The voltage-gated proton channel: a riddle, wrapped in a mystery, inside an enigma. *Biochemistry*. 54:3250–3268. <https://doi.org/10.1021/acs.biochem.5b00353>
- DeCoursey, T.E. 2017. CrossTalk proposal: Proton permeation through Hv1 requires transient protonation of a conserved aspartate in the S1 transmembrane helix. *J. Physiol.* 595:6793–6795. <https://doi.org/10.1113/JP274495>
- DeCoursey, T.E. 2018. Voltage and pH sensing by the voltage-gated proton channel, Hv1. *J. R. Soc. Interface.* 15:20180108. <https://doi.org/10.1098/rsif.2018.0108>
- DeCoursey, T.E., and V.V. Cherny. 1993. Potential, pH, and arachidonate gate hydrogen ion currents in human neutrophils. *Biophys. J.* 65:1590–1598. [https://doi.org/10.1016/S0006-3495\(93\)81198-6](https://doi.org/10.1016/S0006-3495(93)81198-6)
- DeCoursey, T.E., and V.V. Cherny. 1995. Voltage-activated proton currents in membrane patches of rat alveolar epithelial cells. *J. Physiol.* 489:299–307. <https://doi.org/10.1113/jphysiol.1995.sp021051>
- DeCoursey, T.E., and V.V. Cherny. 1997. Deuterium isotope effects on permeation and gating of proton channels in rat alveolar epithelium. *J. Gen. Physiol.* 109:415–434. <https://doi.org/10.1085/jgp.109.4.415>
- DeCoursey, T.E., and V.V. Cherny. 1998. Temperature dependence of voltage-gated H⁺ currents in human neutrophils, rat alveolar epithelial cells, and mammalian phagocytes. *J. Gen. Physiol.* 112:503–522. <https://doi.org/10.1085/jgp.112.4.503>
- DeCoursey, T.E., D. Morgan, and V.V. Cherny. 2003. The voltage dependence of NADPH oxidase reveals why phagocytes need proton channels. *Nature*. 422:531–534. <https://doi.org/10.1038/nature01523>
- DeCoursey, T.E., D. Morgan, B. Musset, and V.V. Cherny. 2016. Insights into the structure and function of Hv1 from a meta-analysis of mutation studies. *J. Gen. Physiol.* 148:97–118. <https://doi.org/10.1085/jgp.201611619>
- Demaurex, N., S. Grinstein, M. Jaconi, W. Schlegel, D.P. Lew, and K.H. Krause. 1993. Proton currents in human granulocytes: regulation by membrane potential and intracellular pH. *J. Physiol.* 466:329–344.
- Dudev, T., B. Musset, D. Morgan, V.V. Cherny, S.M.E. Smith, K. Mazmanian, T.E. DeCoursey, and C. Lim. 2015. Selectivity mechanism of the voltage-gated proton channel, Hv1. *Sci. Rep.* 5:10320. <https://doi.org/10.1038/srep10320>
- Gordienko, D.V., M. Tare, S. Parveen, C.J. Fenech, C. Robinson, and T.B. Bolton. 1996. Voltage-activated proton current in eosinophils from human blood. *J. Physiol.* 496:299–316. <https://doi.org/10.1113/jphysiol.1996.sp021686>
- Gu, X., and H. Sackin. 1995. Effect of pH on potassium and proton conductance in renal proximal tubule. *Am. J. Physiol.* 269:F289–F308. <https://doi.org/10.1152/ajprenal.1995.269.3.F289>
- Henderson, L.M., J.B. Chappell, and O.T.G. Jones. 1987. The superoxide-generating NADPH oxidase of human neutrophils is electrogenic and associated with an H⁺ channel. *Biochem. J.* 246:325–329. <https://doi.org/10.1042/bj2460325>
- Kapus, A., R. Romanek, A.Y. Qu, O.D. Rotstein, and S. Grinstein. 1993. A pH-sensitive and voltage-dependent proton conductance in the plasma membrane of macrophages. *J. Gen. Physiol.* 102:729–760. <https://doi.org/10.1085/jgp.102.4.729>
- Katoh, K., and D.M. Standley. 2013. MAFFT multiple sequence alignment software version 7: improvements in performance and usability. *Mol. Biol. Evol.* 30:772–780. <https://doi.org/10.1093/molbev/mst010>
- Koch, H.P., T. Kurokawa, Y. Okochi, M. Sasaki, Y. Okamura, and H.P. Larsson. 2008. Multimeric nature of voltage-gated proton channels. *Proc. Natl. Acad. Sci. USA.* 105:9111–9116. <https://doi.org/10.1073/pnas.0801553105>
- Kulleperuma, K., S.M.E. Smith, D. Morgan, B. Musset, J. Holyoake, N. Chakrabarti, V.V. Cherny, T.E. DeCoursey, and R. Pom es. 2013. Construction and validation of a homology model of the human voltage-gated proton channel hHv1. *J. Gen. Physiol.* 141:445–465. <https://doi.org/10.1085/jgp.201210856>
- Kuno, M., H. Ando, H. Morihata, H. Sakai, H. Mori, M. Sawada, and S. Oiki. 2009. Temperature dependence of proton permeation through a voltage-gated proton channel. *J. Gen. Physiol.* 134:191–205. <https://doi.org/10.1085/jgp.200910213>
- Lee, S.Y., J.A. Letts, and R. Mackinnon. 2008. Dimeric subunit stoichiometry of the human voltage-dependent proton channel Hv1. *Proc. Natl. Acad. Sci. USA.* 105:7692–7695. <https://doi.org/10.1073/pnas.0803277105>
- Li, Q., R. Shen, J.S. Treger, S.S. Wanderling, W. Milewski, K. Siwowska, F. Bezanilla, and E. Perozo. 2015. Resting state of the human proton channel dimer in a lipid bilayer. *Proc. Natl. Acad. Sci. USA.* 112:E5926–E5935. <https://doi.org/10.1073/pnas.1515043112>
- Morgan, D., B. Musset, K. Kulleperuma, S.M.E. Smith, S. Rajan, V.V. Cherny, R. Pom es, and T.E. DeCoursey. 2013. Peregrination of the selectivity filter delineates the pore of the human voltage-gated proton channel hHv1. *J. Gen. Physiol.* 142:625–640. <https://doi.org/10.1085/jgp.201311045>
- Murphy, R., and T.E. DeCoursey. 2006. Charge compensation during the phagocyte respiratory burst. *Biochim. Biophys. Acta.* 1757:996–1011. <https://doi.org/10.1016/j.bbabi.2006.01.005>
- Musset, B., V.V. Cherny, D. Morgan, Y. Okamura, I.S. Ramsey, D.E. Clapham, and T.E. DeCoursey. 2008. Detailed comparison of expressed and native voltage-gated proton channel currents. *J. Physiol.* 586:2477–2486. <https://doi.org/10.1113/jphysiol.2007.149427>
- Musset, B., S.M.E. Smith, S. Rajan, V.V. Cherny, S. Sujai, D. Morgan, and T.E. DeCoursey. 2010. Zinc inhibition of monomeric and dimeric proton channels suggests cooperative gating. *J. Physiol.* 588:1435–1449. <https://doi.org/10.1113/jphysiol.2010.188318>

- Musset, B., S.M.E. Smith, S. Rajan, D. Morgan, V.V. Cherny, and T.E. DeCoursey. 2011. Aspartate112 is the selectivity filter of the human voltage-gated proton channel. *Nature*. 480:273–277. <https://doi.org/10.1038/nature10557>
- Nordström, T., O.D. Rotstein, R. Romanek, S. Asotra, J.N. Heersche, M.F. Manolson, G.F. Brisseau, and S. Grinstein. 1995. Regulation of cytoplasmic pH in osteoclasts. Contribution of proton pumps and a proton-selective conductance. *J. Biol. Chem.* 270:2203–2212. <https://doi.org/10.1074/jbc.270.5.2203>
- Ramsey, I.S., Y. Mokrab, I. Carvacho, Z.A. Sands, M.S.P. Sansom, and D.E. Clapham. 2010. An aqueous H⁺ permeation pathway in the voltage-gated proton channel Hv1. *Nat. Struct. Mol. Biol.* 17:869–875. <https://doi.org/10.1038/nsmb.1826>
- Rodriguez, J.D., S. Haq, T. Bachvaroff, K.F. Nowak, S.J. Nowak, D. Morgan, V.V. Cherny, M.M. Sapp, S. Bernstein, A. Bolt, et al. 2017. Identification of a vacuolar proton channel that triggers the bioluminescent flash in dinoflagellates. *PLoS One*. 12:e0171594. <https://doi.org/10.1371/journal.pone.0171594>
- Sakata, S., N. Miyawaki, T.J. McCormack, H. Arima, A. Kawanabe, N. Özkucur, T. Kurokawa, Y. Jinno, Y. Fujiwara, and Y. Okamura. 2016. Comparison between mouse and sea urchin orthologs of voltage-gated proton channel suggests role of S3 segment in activation gating. *Biochim. Biophys. Acta*. 1858:2972–2983. <https://doi.org/10.1016/j.bbame.2016.09.008>
- Schilling, T., A. Gratopp, T.E. DeCoursey, and C. Eder. 2002. Voltage-activated proton currents in human lymphocytes. *J. Physiol.* 545:93–105. <https://doi.org/10.1113/jphysiol.2002.028878>
- Schrenzel, J., D.P. Lew, and K.H. Krause. 1996. Proton currents in human eosinophils. *Am. J. Physiol.* 271:C1861–C1871. <https://doi.org/10.1152/ajpcell.1996.271.6.C1861>
- Smith, S.M.E., D. Morgan, B. Musset, V.V. Cherny, A.R. Place, J.W. Hastings, and T.E. DeCoursey. 2011. Voltage-gated proton channel in a dinoflagellate. *Proc. Natl. Acad. Sci. USA*. 108:18162–18167. <https://doi.org/10.1073/pnas.1115405108>
- Szteyn, K., W. Yang, E. Schmid, F. Lang, and E. Shumilina. 2012. Lipopolysaccharide-sensitive H⁺ current in dendritic cells. *Am. J. Physiol. Cell Physiol.* 303:C204–C212. <https://doi.org/10.1152/ajpcell.00059.2012>
- Takeshita, K., S. Sakata, E. Yamashita, Y. Fujiwara, A. Kawanabe, T. Kurokawa, Y. Okochi, M. Matsuda, H. Narita, Y. Okamura, and A. Nakagawa. 2014. X-ray crystal structure of voltage-gated proton channel. *Nat. Struct. Mol. Biol.* 21:352–357. <https://doi.org/10.1038/nsmb.2783>
- Thomas, S., V.V. Cherny, D. Morgan, L.R. Artinian, V. Rehder, S.M.E. Smith, and T.E. DeCoursey. 2018. Exotic properties of a voltage-gated proton channel from the snail *Helisoma trivolvis*. *J. Gen. Physiol.* <https://doi.org/10.1085/201711967>
- Tombola, F., M.H. Ulbrich, and E.Y. Isacoff. 2008. The voltage-gated proton channel Hv1 has two pores, each controlled by one voltage sensor. *Neuron*. 58:546–556. <https://doi.org/10.1016/j.neuron.2008.03.026>
- van Keulen, S.C., E. Gianti, V. Carnevale, M.L. Klein, U. Rothlisberger, and L. Delemotte. 2017. Does proton conduction in the voltage-gated H⁺ channel hHv1 involve Grothuss-like hopping via acidic residues? *J. Phys. Chem. B*. 121:3340–3351. <https://doi.org/10.1021/acs.jpcc.6b08339>
- Walther, D., and P. Argos. 1996. Intrahelical side chain-side chain contacts: the consequences of restricted rotameric states and implications for helix engineering and design. *Protein Eng.* 9:471–478. <https://doi.org/10.1093/protein/9.6.471>